Bouncing ball with a finite restitution: Chattering, locking, and chaos

J. M. Luck*
Service de Physique Théorique, Centre d'Etudes de Saclay, 91191 Gif-sur-Yvette CEDEX, France

Anita Mehta†
Interdisciplinary Research Centre in Materials, University of Birmingham, Edgbaston, Birmingham B15 2TT, United Kingdom
(Received 2 June 1993)

We study the dynamic evolution of a bouncing ball on a vibrating platform, such as the membrane of a loudspeaker, as a function of its coefficient of restitution α and demonstrate primarily that the presence of chaos in this system is by no means inevitable and its development is by no means obvious. Indeed, we show that generic trajectories starting under experimental conditions terminate in a region of "chattering" (where the memory of earlier dynamics is lost), before repeating themselves in a periodic way. As a consequence, except possibly for the strictly elastic case ($\alpha=1$), the evolution to chaos via a period-doubling route will not be observed. Our arguments are corroborated by numerical studies, concerning especially the divergence of the mean period of generic trajectories as the elastic limit is approached ($\alpha\to 1$).

PACS number(s): 46.10.+z, 03.20.+i, 05.45.+b

I. INTRODUCTION

The dynamical behavior of a bouncing ball on a vibrating platform, e.g., a loudspeaker membrane, has, since the seminal work of Fermi [1], intrigued physicists and been a fecund source of theoretical and experimental investigations [2–14]. Since in practice such balls are neither perfectly elastic nor perfectly inelastic, one can safely assume that the bulk of the experimental literature at least concerns the case where the coefficient of restitution α takes values between 0 and 1. It is therefore astonishing that there has hitherto been a rather cavalier treatment of the dynamics of the ball with finite restitution, in the ubiquity of observed or calculated "chaotic" behavior, since, as we show in this paper, *generic trajectories are periodic.*

Indeed, we find that there is a "locking" region in phase space, where the ball is relaunched to recommence its earlier trajectory, and predict therefore that *the period-doubling route to chaos should not be observed.*

In earlier theoretical treatments, all of which have been based on (variants of) the Chirikov "high-bounce" approximation [4], chaos was "seen" to be present for the partially elastic bouncing ball, as well as for the completely inelastic bouncing ball, simply because the motion of the platform was ignored. It is easy to see (as we demonstrated in earlier work [15]) that this approximation leads to erroneous results for the completely inelastic bouncing ball. The gist of our argument is as follows: when the ball lands in the *absorbing region* of the platform cycle (where it is kinematically impossible for it to be launched upwards), it "sticks" to the platform because α is strictly zero. It is then relaunched in the beginning of the *transmitting region* of the next cycle, with zero relative velocity. This periodic relauching under identical kinematic conditions and the resulting interruption of the period-doubling sequence are consequences of the *complete* inelasticity of the ball.

This line of reasoning might suggest that when α is not strictly zero, i.e., when the ball is able to rebound in an erstwhile absorbing region and possibly "hop" across to a transmitting region, the period-doubling sequence might continue to evolve, resulting in chaos. The point of this paper is to state that this is *not* the case, except possibly at $\alpha=1$ (in this elastic limit, the energy of the ball is unbounded, and the analysis of the dynamics is difficult for obvious reasons). Although it is possible for the ball with finite restitution to hop its way out of many absorbing regions, we show that generic trajectories end in *complete chattering,* or *locking,* i.e., the ball hops infinitely many times in an absorbing region without ever getting to a transmitting region, since the hop amplitudes decay exponentially. Thus the period-doubling route to chaos is never observable for generic trajectories for *any* α less than 1.

This still leaves outstanding the question of why chaos is "observed" experimentally. The answer is that the periodic trajectories mentioned above are very long and complicated, especially near the elastic limit ($\alpha\to 1$). It is thus very plausible that in experimentally observable times neighboring trajectories will diverge from each other's vicinity, so that some manifestation of chaos, such as a positive Lyapunov exponent, will be observed. Alternatively, a sequence of such periodic trajectories, when juxtaposed, will be difficult to distinguish from a chaotic trajectory, at least from an experimental point of view. Finally, since real balls may not always be characterizable by a single scalar coefficient of restitution, it is possible that complicated tensorial aspects to their elastic properties could account for experimentally observed chaos to date.

The plan of this paper is as follows. In Sec. II we write down the dynamical equations for the ball with partial elasticity. We proceed to analyze local aspects of the ex-

act map such as fixed-point trajectories and their stability and the evolution of the period-doubling cascade. We show also that in the vicinity of fixed-point trajectories, our rescaled dynamical equations are equivalent to the Hénon map. Next, in Sec. III we do a global analysis and state our rather surprising results for this system. We investigate chattering and locking regions, the conditions under which chaos is observed, and the nature of a generic trajectory, thus building up a physical picture of the bouncing ball with finite restitution. From a quantitative point of view, we obtain a "critical" law of divergence of the mean number of collisions in a period and of its duration, as the elastic regime is approached. In the discussion section (Sec. IV), we summarize our results and mention future directions of research.

II. LOCAL ANALYSIS

The system under investigation consists of a ball on a harmonically vibrating platform; the position of the latter at time t is given by

$$s(t)=A\sin\omega t \ . \tag{2.1}$$

The partially elastic collisions of the ball with the platform are described by a restitution coefficient $0\le\alpha<1$ (the limit case $\alpha=0$ corresponds to the completely inelastic regime, considered in our previous work [15]) and the gravitational acceleration g provides the "restoring force" on the ball in flight.

A. Dynamical equations

Throughout this paper, we will use dimensionless units, measuring time in units of the period $T=2\pi/\omega$ of the platform's oscillations and accelerations in units of $g/2$. In keeping with this, velocities will be expressed in units of $\pi g/\omega$ and positions in units of $2\pi^2 g/\omega^2$. The rescaled quantities representing the motion of the platform are then $\tau=t/T=\omega t/(2\pi)$ and $S=\omega^2 s/(2\pi^2 g)$. Equation (2.1) thus reads

$$S(\tau)=\frac{\Gamma}{2\pi}\sin(2\pi\tau) \ . \tag{2.2}$$

The reduced acceleration $\Gamma=A\omega^2/(\pi g)$ and the restitution coefficient α are the two dimensionless control parameters of the problem.

The height of the ball $X(\tau)$ during its flight between any two ball-platform collisions is described by the following parabolic equation:

$$X(\tau)=X_0+V_0(\tau-\tau_0)-(\tau-\tau_0)^2 \ , \tag{2.3}$$

where τ_0 is the last time at which the ball was launched from the platform, $X_0=S(\tau_0)$ and

$$V_0=W_0+\frac{dS}{d\tau_0}=W_0+\Gamma\cos(2\pi\tau_0) \ , \tag{2.4}$$

where $W_0>0$ is the relative "takeoff" velocity of the ball.

The next collision time is the smallest solution $\tau_1>\tau_0$ of $\Delta(\tau)=0$, where

$$\begin{aligned}\Delta(\tau)&=X(\tau)-S(\tau)\\&=\frac{\Gamma}{2\pi}[\sin(2\pi\tau_0)-\sin(2\pi\tau_1)]\\&\quad+[W_0+\Gamma\cos(2\pi\tau_0)](\tau_1-\tau_0)-(\tau_1-\tau_0)^2\end{aligned} \tag{2.5}$$

is the relative height of the ball above the platform.

The relative "landing" velocity

$$\begin{aligned}W_1^{(-)}=\frac{d\Delta}{d\tau_1}&=W_0-2(\tau_1-\tau_0)\\&\quad+\Gamma[\cos(2\pi\tau_0)-\cos(2\pi\tau_1)]\end{aligned} \tag{2.6}$$

is negative, since we have $\Delta(\tau)>0$ during the flight, i.e., $\tau_0<\tau<\tau_1$. Because the collision is partially elastic, i.e., $0<\alpha<1$, the ball bounces back immediately at $\tau=\tau_1$, with a positive relative velocity given by

$$W_1=-\alpha W_1^{(-)} \ . \tag{2.7}$$

The above equations (2.5)–(2.7) define an implicit dynamical mapping

$$T:\ (\tau_0,W_0)\mapsto(\tau_1,W_1) \ , \tag{2.8}$$

where α and Γ are two dimensionless control parameters. A forward orbit $\{(\tau_k,W_k)\}$, describing one possible history of the ball, can be generated by iterating the above dynamical equations, starting from arbitrary initial conditions. It will be convenient for some purposes to fold the time variable τ modulo the unit period of the platform, considering thus the reduced phase space $(0\le\tau\le1, W>0)$, which has the topology of a half-cylinder.

The rest of this section is devoted to a local analysis of the dynamical equations derived above, with $\alpha>0$, including the study of fixed-point trajectories, period-doubling solutions, and their stability.

B. Fixed-point trajectories

A fixed-point trajectory is such that the time of flight of the ball is an integer number $m\ge1$ of platform cycles. With the notation $(\tau_0=\tau_*, W_0=W_*)$, we have $(\tau_1=\tau_*+m, W_1=W_*)$. The motion is then periodic, i.e., the orbit is described by $(\tau_k=\tau_*+km, W_k=W_*)$. We also introduce the value of the absolute velocity as $V_0=V_*$. Equations (2.5)–(2.7) easily yield the conditions

$$\Gamma\cos(2\pi\tau_*)=\frac{1-\alpha}{1+\alpha}m, \quad W_*=\frac{2\alpha}{1+\alpha}m, \quad V_*=m \ . \tag{2.9}$$

This result characterizes all fixed-point periodic orbits, with the following qualifying remarks: First, only stable trajectories have a chance to be observed. The study of the stability of fixed-point solutions will be presented shortly. Second, a *transmission condition,* to be derived in Sec. III B has to be imposed in order to ensure that there is not a premature ball-platform collision in the launch cycle. Let us anticipate that this condition reads

$$W>W_A(\tau) \ , \tag{2.10}$$

where $W_A(\tau)$ will be determined in Sec. III B.

In order to know whether the fixed-point solution (2.9) is linearly stable, we insert perturbed initial values of the form $(\tau_0=\tau_*+\delta\tau_0, W_0=W_*+\delta W_0)$ into the dynamical equations (2.5)–(2.7). To linear order, the perturbations after one period read

$$\begin{bmatrix}\delta\tau_1\\ \delta W_1\end{bmatrix}=\begin{bmatrix}1-(1+\alpha)\sigma & (1+\alpha)/2\\ 2\alpha(1+\alpha)\sigma(\sigma-1) & \alpha^2-\alpha(1+\alpha)\sigma\end{bmatrix}\begin{bmatrix}\delta\tau_0\\ \delta W_0\end{bmatrix}, \tag{2.11}$$

with

$$\sigma=\pi\Gamma\sin(2\pi\tau_*)\ . \tag{2.12}$$

The fixed-point periodic trajectory is stable if and only if both eigenvalues of the above matrix are smaller than unity in absolute value. We thus get the following condition:

$$0<\sigma<\frac{2(1+\alpha^2)}{(1+\alpha)^2}\ , \tag{2.13}$$

i.e., in terms of Γ,

$$\frac{1-\alpha}{1+\alpha}m<\Gamma<\left\{\left[\frac{1-\alpha}{1+\alpha}m\right]^2+\left[\frac{2(1+\alpha^2)}{\pi(1+\alpha)^2}\right]^2\right\}^{1/2}. \tag{2.14}$$

The stable fixed-point orbits build therefore equally spaced *bands,* one for every integer period m, situated around $\Gamma=(1-\alpha)m/(1+\alpha)$. For m large, the bands get narrower, since their widths shrink according to

$$\delta\Gamma\approx\frac{2(1+\alpha^2)^2}{\pi^2(1+\alpha)^3(1-\alpha)m}\ . \tag{2.15}$$

The region of stability of fixed-point orbits for finite α is a continuous deformation of the situation in the completely inelastic case ($\alpha=0$), described in Ref. [15].

When a fixed-point solution becomes unstable, it can undergo a complete or an incomplete period-doubling cascade. This question is complicated by the existence of a transmission condition, as stated above. A full analysis of the period-doubling sequence will only be performed in the large-Γ regime, where the dynamical mapping can be simplified as explained below.

C. The scaling region: Connections with the Hénon map

The dynamical mapping (2.8) can be greatly simplified in the large-m regime, in the vicinity of the fixed-point trajectories described above. This can be shown by performing the following $1/m$ expansion of the dynamical variables around the fixed-point solution (2.9)

$$\begin{aligned}\Gamma&=\frac{1-\alpha}{1+\alpha}m+\frac{\gamma}{\pi^2(1+\alpha)^3(1-\alpha)m}+\cdots\ ,\\ \tau&=\frac{y}{2\pi^2(1-\alpha^2)m}+\cdots\ ,\\ V&=m+\frac{z}{\pi^2(1+\alpha)^2(1-\alpha)m}+\cdots\ ,\\ W&=\frac{2\alpha}{1+\alpha}m+\frac{(1+\alpha)z+y^2/2-\gamma}{\pi^2(1+\alpha)^3(1-\alpha)m}+\cdots\ .\end{aligned} \tag{2.16}$$

These expansions involve two rescaled dynamical variables y and z, whereas γ is a rescaled control parameter. Powers of $(1\pm\alpha)$ have been inserted for further convenience. The expression for W is a consequence of the other definitions.

The dynamical equations (2.5)–(2.7) become, when expanded to first nontrivial order for large m, the following polynomial map in two variables:

$$P:\ \begin{bmatrix}y\\ z\end{bmatrix}\mapsto\begin{bmatrix}y'=y+z\\ z'=\gamma+\alpha^2z-(y+z)^2/2\end{bmatrix}, \tag{2.17}$$

where α and γ are two control parameters.

We also have to determine the rescaled form of the transmission condition (2.10). By inserting the expansion (2.16) into Eq. (3.10), it can be shown that the upper critical value of τ, for which $\theta=\tau$, and hence $W_A=0$, is very close to $\tau=1$ for large m. More precisely, it corresponds to

$$y_c=(1+\alpha)^2\ . \tag{2.18}$$

Furthermore, the scaling form of the limiting velocity W_A reads

$$W_A=\begin{cases}0, & y\geq y_c\\ \dfrac{3(y_c-y)^2}{8\pi^2(1+\alpha)^3(1-\alpha)m}, & y\leq y_c\ .\end{cases} \tag{2.19}$$

The role of the transmission condition (2.10) will be discussed in Sec. II D.

It is worth noticing that the transformation P can be recast, by means of an inhomogeneous linear change of coordinates, in the form of the celebrated Hénon map ([16]; see Ref. [17] for a review)

$$H:\ \begin{bmatrix}X\\ Y\end{bmatrix}\mapsto\begin{bmatrix}X'=1-aX^2+Y\\ Y'=bX\end{bmatrix}, \tag{2.20}$$

with the following values of the parameters:

$$a=\gamma/2-(1+\alpha^2)^2/4,\quad b=-\alpha^2\ . \tag{2.21}$$

A peculiarity of the present case concerns the unusual sign of the Jacobian of the map H, which reads

$$J=\frac{\partial(y',z')}{\partial(y,z)}=\alpha^2>0\ , \tag{2.22}$$

whereas the Hénon map has usually been studied for positive values of the parameter b, so that $J=-b<0$.

D. Period doubling, chaos, and their limitations

1. *The completely inelastic case: $\alpha=0$*

Let us first look at the case of completely inelastic collisions. In this situation ($\alpha=0$), the relative velocities W vanish identically. Equation (2.16) therefore implies $z=\gamma-y^2/2$, and the rescaled map (2.17) becomes the following quadratic map in one variable:

$$P_0:\ y\mapsto y'=\gamma+y-y^2/2\ , \tag{2.23}$$

on which the transmission condition (2.10) imposes the inequality

$$y \geq 1 \ . \tag{2.24}$$

Indeed, the first alternative of Eq. (2.19) has to be obeyed, and we have $y_c = 1$ for $\alpha = 0$. Equivalent results were already presented in our previous work [15].

The transformation (2.23) can be brought to either of the following canonical forms for quadratic maps (see Ref. [18] for a review):

$$P_1: \ u \mapsto u' = u^2 + c \ \text{ with } c = \tfrac{1}{4} - \gamma/2 \ , \tag{2.25}$$

via the change of variable $z = (1-y)/2$, and

$$P_2: \ x \mapsto x' = 1 - \mu x^2 \ \text{ with } \mu = \gamma/2 - \tfrac{1}{4} \ , \tag{2.26}$$

via the change of variable $x = (y-1)/(\gamma - 1/2)$.

It is well-known that the quadratic map (2.23), (2.25), and (2.26) undergoes a sequence of period-doubling bifurcations [19].

In the present case, we shall say that an attractor, such as a 2^k-cycle $\{y_1, \ldots y_{2^k}\}$, is *visible* if (i) the attractor is linearly stable and (ii) it is entirely contained in the allowed region of y space, i.e., $\min \{y_l : 1 \leq l \leq 2^k\} \geq 1$.

It turns out that the visible attractors of the map (2.23) are the following: (i) a fixed point $y = (2\gamma)^{1/2}$, stable for $\gamma_1 = 0 < \gamma < \gamma_2 = 2$ and visible for $1/2 < \gamma < 2$; and (ii) a two-cycle $(y_1, y_2) = 2 \pm [2(\gamma - 2)]^{1/2}$, stable for $\gamma_2 = 2 < \gamma < \gamma_4 = 3$ and visible for $2 < \gamma < \frac{5}{2}$. We notice that the domain of stability of the fixed point matches the more general expression (2.14).

2. *The case $\alpha \ll 1$*

We now extend the above results to small nonzero values of the restitution coefficient α. The expansion (2.16) of the relative velocity W suggests that α only enters the problem through the following scaling variable:

$$\beta = \alpha \Gamma^2 \ , \tag{2.27}$$

in the large-Γ regime, which is in any case the only regime we will examine in depth.

We are thus led to consider the *scaling region* ($\alpha \ll 1, \Gamma \gg 1$), keeping the variable β fixed. In this situation, the z variable can still be ignored, since $z = \gamma - y^2/2 + O(\alpha^2)$, by virtue of Eq. (2.17). Furthermore, the dynamics of the remaining y variable is approximately given by the $\alpha = 0$ map P_0, introduced in Eq. (2.23).

The only nontrivial place where the scaling parameter β enters is the transmission condition. Relative velocities can be approximated by the term of order m in the expansion (2.16). Since W_A is given by Eq. (2.19), the inequality (2.10) assumes the simple form

$$y > y_c(\beta) \ , \tag{2.28}$$

with

$$y_c(\beta) = 1 - 4\pi(\beta/3)^{1/2}, \ \text{ i.e., } \ \beta = \frac{3}{16\pi^2}(1 - y_c)^2 \ . \tag{2.29}$$

This condition generalizes the inequality (2.24) to nonzero values of α in the scaling region.

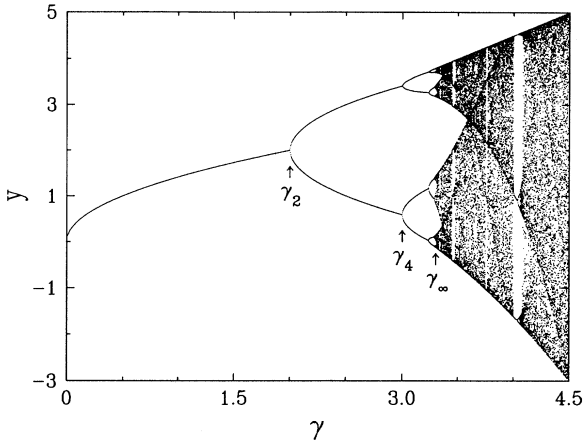

FIG. 1. Plot of the attractor of the quadratic map P_0 of Eq. (2.23), acting on the y variable in the completely inelastic case, against the rescaled control parameter γ. A few remarkable values of γ, discussed in the text, are indicated.

When β is increased from zero to larger and larger values, more and more of the period-doubling bifurcations of the map P_0 become visible. Figure 1 illustrates this discussion. Besides the fixed point and the two-cycle, which are already visible in the completely inelastic case ($\beta = 0$), (i) a four-cycle is stable for $\gamma_4 = 3 < \gamma < \gamma_8 = 3.236\,198$ and becomes visible for $\beta > \beta_4 = 3(\sqrt{2} - 1)^2/(16\pi^2) = 0.003\,259\,5$; (ii) similarly, an eight-cycle is stable for $\gamma_8 = 3.236\,198 < \gamma < \gamma_{16} = 3.288\,092$ and becomes visible for $\beta > \beta_8 = 0.018\,880$, and so on; (iii) the period-doubling cascade accumulates onto the Myrberg point, situated at $\gamma_\infty = 3.302\,310$ [18]. The corresponding aperiodic attractor extends from $y_{\min} = -0.124\,161$ to $y_{\max} = 3.802\,310$.

The first point at which an aperiodic orbit, i.e., *chaos*, can be observed is therefore $\beta = \beta_\infty = 3(1 - y_{\min})^2/(16\pi^2) = 0.024\,008$. This last number can be interpreted as follows. The partially elastic bouncing ball can only exhibit chaos when the restitution coefficient is large enough, namely for $\beta > \beta_\infty$, or

$$\alpha > \frac{0.024\,008}{\Gamma^2} \ , \tag{2.30}$$

in the large-Γ regime. Notice that the condition (2.30) involves a very small numerical factor.

It will, however, become clear in the following that this route to chaos via a period-doubling cascade is very unlikely to be observed; this is because of the existence of a locking region in phase space, in which trajectories lose their memory. We will address these issues in the next section.

III. GLOBAL ANALYSIS

We now turn to the analysis of some global aspects of the dynamics of the partially elastic bouncing ball, such as the typical fate of a generic trajectory. This discus-

sion, to be presented in Sec. III D, requires some preliminary technicalities which follow.

A. The volume of phase space

The relative velocity W as well as the duration $\delta\tau=\tau_1-\tau_0$ of flight of the ball remain bounded as long as the restitution coefficient α is less than unity. We will give an elementary proof of this fact and obtain rough estimates of the maximal values $W_{\max}$ and $\delta\tau_{\max}$. On the other hand, as mentioned earlier, we can consider a reduced phase space ($0\le\tau\le 1, W>0$), defined by making the time variable τ compact. The dynamically accessible portion of this phase space has therefore a finite volume of order $W_{\max}$.

A rough upper bound $W_{\max}$ of the relative velocities can be derived as follows. We put simple bounds on the dynamical equations (2.5)–(2.7), by replacing the trigonometric lines by their extremal values ± 1,

$$W_1\le\alpha[2(\tau_1-\tau_0)-W_0+2\Gamma]\ , \tag{3.1a}$$

$$\Delta(\tau_1)\le\Gamma/\pi+V_0(\tau_1-\tau_0)-(\tau_1-\tau_0)^2\ , \tag{3.1b}$$

$$V_0\le W_0+\Gamma\ . \tag{3.1c}$$

For fixed initial conditions (τ_0, W_0), we can use Eqs. (3.1b) and (3.1c) to derive an upper bound for $\Delta(\tau_1)$, involving W_0, and then use Eq. (3.1a) to get an upper bound for W_1, namely

$$W_1\le\alpha\{3\Gamma+[(W_0+\Gamma)^2+4\Gamma/\pi]^{1/2}\}\ . \tag{3.2}$$

After a transient regime, i.e., for k large enough, the relative velocities W_k are bounded by the fixed-point value $W_{\max}$ defined by setting $W_1=W_0=W_{\max}$ in Eq. (3.2). We thus get

$$W_{\max}=\frac{\alpha}{1-\alpha^2}\{(3+\alpha)\Gamma+[4(1-\alpha^2)\Gamma/\pi+(1+3\alpha)^2\Gamma^2]^{1/2}\}\ . \tag{3.3}$$

We can then derive from Eqs. (3.1) a bound on the duration $\delta\tau_{\max}$ of a ball's flight, as the solution of the quadratic equation

$$\delta\tau_{\max}^2-(W_{\max}+\Gamma)\delta\tau_{\max}-\Gamma/\pi=0\ . \tag{3.4}$$

We obtain after some algebra

$$\delta\tau_{\max}=\frac{1}{2(1-\alpha)}\{(1+3\alpha)\Gamma+[4(1-\alpha^2)\Gamma/\pi+(1+3\alpha)^2\Gamma^2]^{1/2}\}\ . \tag{3.5}$$

The above expressions (3.3)–(3.5) are only meant as rough guides. Nevertheless, their large-Γ behavior, namely

$$W_{\max}\approx\frac{4\alpha}{1-\alpha}\Gamma,\quad \delta\tau_{\max}\approx\frac{1+3\alpha}{1-\alpha}\Gamma\ , \tag{3.6}$$

yields simple estimates which capture the essential expected features. Both estimates are proportional to Γ and diverge as the elastic limit is approached ($\alpha\to 1$). Moreover, $W_{\max}$ vanishes proportionally to α for small α. Absolute prefactors, such as the constant 4 in $W_{\max}$, are certainly overestimated.

B. Absorbing and transmitting regions

One of the main outcomes of our previous work [15] was that one cycle of the platform could be decomposed into a transmitting and an absorbing region, according, respectively, to whether or not long flights (with duration $\tau_1-\tau_0\sim\Gamma$ for large Γ) were allowed.

This concept is generalized as follows in the present case ($\alpha>0$). For any takeoff time $0<\tau_0<1$, there is a limiting relative velocity denoted by $W_A(\tau_0)$, such that (i) for $W_0<W_A(\tau_0)$, there is an "early" ball-platform collision either in the launch cycle or in the beginning of the next one, i.e., $\tau_1\le\frac{5}{4}$. This is the *absorbing region* of phase space; and (ii) for $W_0>W_A(\tau_0)$, the ball is launched with a strong enough impulse that it can overcome the next barrier, viz. that of the platform's largest upward oscillation which takes place around $\tau=\frac{5}{4}$. This is the *transmitting region* of phase space.

In the transmitting region, and in the large-Γ regime, the dynamics of the ball can be described by the so-called *high-bounce approximation,* which consists of neglecting the initial positions of the ball and of the platform (i.e., the sine functions) in the expression (2.5) of their relative position [4]. We thus obtain the following simple and explicit formula

$$\tau_1\approx\tau_0+W_0+\Gamma\cos(2\pi\tau_0)\ . \tag{3.7}$$

Let us now determine the limiting initial condition $W=W_A(\tau_0)$ which demarcates between the transmitting and absorbing regions of phase space. Let $\theta(\tau_0)$ denote the value of τ_1 corresponding to this marginal situation, for which the platform and the ball have "grazing" or tangential trajectories at $\tau=\theta$, namely

$$\begin{aligned}\Delta&=\frac{\Gamma}{2\pi}[\sin(2\pi\tau_0)-\sin(2\pi\theta)]\\&\quad+[W_A+\Gamma\cos(2\pi\tau_0)](\theta-\tau_0)-(\theta-\tau_0)^2=0\ ,\\ \frac{d\Delta}{d\theta}&=W_A-2(\theta-\tau_0)+\Gamma[\cos(2\pi\tau_0)-\cos(2\pi\theta)]=0\ .\end{aligned} \tag{3.8}$$

These two equations determine $\theta(\tau_0)$ and $W_A(\tau_0)$ for $\frac{1}{4}<\tau_0<1$.

For large Γ, we have the somehow simpler expression

$$W_A\approx[\cos(2\pi\theta)-\cos(2\pi\tau_0)]\Gamma\ , \tag{3.9}$$

whereas the equation for $\theta(\tau_0)$ remains implicit, namely

$$\sin(2\pi\tau_0)-\sin(2\pi\theta)+2\pi(\theta-\tau_0)\cos(2\pi\theta)=0\ . \tag{3.10}$$

The variations of the ratio W_A/Γ are shown in Fig. 2. This quantity vanishes linearly as $\tau_0\to\frac{1}{4}$ and quadratically as $\tau_0\to 1$, according to

$$W_A\approx\tfrac{3}{2}\pi^2(1-\tau_0)^2\Gamma\ , \tag{3.11}$$

in agreement with the $y\to-\infty$ behavior of the rescaled form (2.19) of the transmission condition.

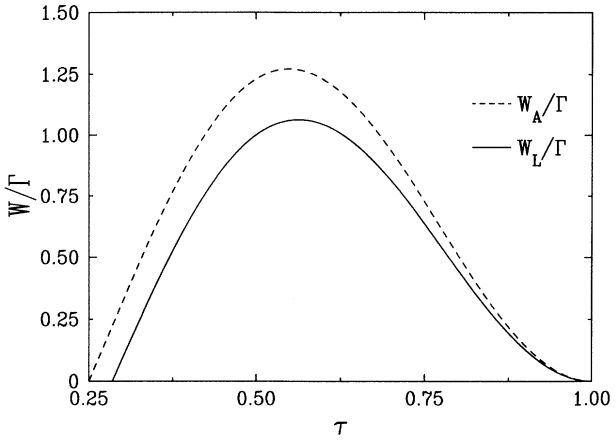

FIG. 2. Plot of the ratios $W_A(\tau)/\Gamma$ and $W_L(\tau)/\Gamma$, against the collision time τ, for $\alpha \ll 1$ and $\Gamma \gg 1$. The absorbing (locking) region of phase space corresponds to relative velocities smaller than W_A (W_L).

The connection with our previous work [15] concerning the completely inelastic case is made as follows. For $\alpha=0$, the relative velocities W_k vanish. The ball can therefore only be launched from the platform for $W_A(\tau_0)=0$, i.e., $\pi\Gamma\sin(2\pi\tau_0)>1$. This last condition is equivalent, as it should be, to requiring that the relative acceleration at takeoff is positive, i.e.,

$$\frac{d^2\Delta}{d\tau_1^2}(\tau_1=\tau_0)=2[\pi\Gamma\sin(2\pi\tau_0)-1]>0\ . \tag{3.12}$$

If this condition is not obeyed, the ball waits on the platform until the beginning of the next cycle. As a consequence, for $\alpha=0$ and in the large-Γ regime, the cycle $0<\tau_0<1$ of the platform is separated into two regions, namely (i) $0<\tau_0<\frac{1}{4}$—when landing in this transmitting region, the ball is immediately relaunched; a long flight results with a duration proportional to Γ, which can be estimated via the high-bounce approximation (3.7); and (ii) $\frac{1}{4}<\tau_0<1$—when landing in this absorbing region, the ball will not perform a long flight, because it will either wait to be relaunched in the next cycle, or will hop i.e., will have a flight time of less than a cycle.

The situation in the partially elastic case is not qualitatively different. The absorbing region is now the area of phase space defined by the inequality $W<W_A(\tau)$.

C. Chattering and locking

For any nonzero value of the restitution coefficient α, the ball will not sit still on the platform if it lands with a positive relative velocity. Nevertheless, if it lands deep enough in the absorbing region of phase space, i.e., $W \ll W_A$, it will perform a large number of smaller and smaller bounces. We refer to this kind of motion as *chattering*.

Chattering will be said to be *complete* if the ball performs an infinity of smaller and smaller bounces in a finite time. This is possible because the relative velocities W_k are approximately reduced by a multiplicative factor of α at each collision, so that the time intervals between collisions can follow a convergent geometrical progression.

Complete chattering, or *locking*, will take place if the relative velocity W_0 is smaller than some threshold value $W_L(\tau_0)$, depending on α and Γ in a complicated fashion. Here again, we will restrict the analysis to the large-Γ regime. The variations of W_L will be studied analytically in the limits $\alpha\to 0$ and $\alpha\to 1$ and numerically in the general case.

For $\alpha\to 0$, the locking condition is equivalent to requiring that τ_1 is less than the beginning of the next cycle, which is the first point at which the ball can be relaunched with an upward acceleration. By inserting $\tau_1=1$ into Eq. (2.5), we obtain

$$W_L(\tau_0)\approx -\left[\cos(2\pi\tau_0)+\frac{\sin(2\pi\tau_0)}{2\pi(1-\tau_0)}\right]\Gamma$$
$$(\Gamma\gg 1,\alpha\ll 1)\ . \tag{3.13}$$

There can only be locking if $W_L>0$, namely for $\tau_{\min}<\tau<1$, where $\tau_{\min}=0.284\,852$. This value is only slightly above the value $\frac{1}{4}$, used throughout in Ref. [15] for the sake of simplicity, and recalled at the end of Sec. III B. It is also worth noticing that the value of W_L in the $\alpha\to 0$ limit is only slightly below the value of W_A. For instance, for $\tau_0=\frac{1}{2}$, we have $W_L/\Gamma=1$, whereas $W_A/\Gamma=1+\cos(2\pi\theta)=1.217\,234$. As $\tau_0\to 1$, W_L vanishes quadratically, just as W_A [see Eq. (3.11)], but with a prefactor $\frac{4}{3}$ instead of $\frac{3}{2}$. Figure 2 shows a plot of both ratios, viz. W_A/Γ and W_L/Γ, in the large-Γ and small-α regime.

In the opposite regime ($\alpha\to 1$), a completely chattering, or locking, trajectory consists of many short hops, with small relative velocities, taking place in the portion of the absorbing region which has negative relative accelerations, i.e., $1/2<\tau<1$. In order to describe such a trajectory in an approximate way, we linearize the dynamical equations as follows:

$$\tau_{k+1}-\tau_k\approx -\frac{W_k}{\pi\Gamma\sin(2\pi\tau_k)},\quad W_{k+1}=\alpha W_k\ . \tag{3.14}$$

To leading order as $\alpha\to 1$, Eq. (3.14) can be solved by going to the continuum limit, i.e., by replacing the difference by a differentiation with respect to a continuous variable k. We thus obtain

$$\cos(2\pi\tau_k)-\cos(2\pi\tau_0)\approx\frac{2W_0}{\lambda\Gamma}(1-e^{-k\lambda})\ , \tag{3.15}$$

with $\lambda=-\ln\alpha\approx 1-\alpha$. The limit $W_L(\tau_0)$ of the locking region corresponds to having $\tau_k\to 1$ as $k\to\infty$. We thus obtain

$$W_L(\tau_0)\approx(1-\alpha)\Gamma\sin^2(\pi\tau_0)$$
$$(\Gamma\gg 1,1-\alpha\ll 1,\tfrac{1}{2}<\tau_0<1)\ . \tag{3.16}$$

The "exact" threshold $W_L(\tau_0)$ for locking can be evaluated, for any values of the parameters α and Γ, by means of a numerical solution of the dynamical equations

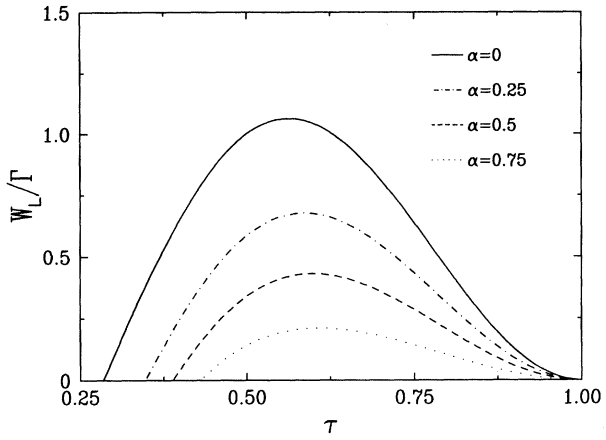

FIG. 3. Plot of the threshold velocity $W_L(\tau)$, below which there is complete chattering, i.e., locking, divided by Γ, in the large-Γ regime, for several values of the restitution coefficient α.

(2.5)–(2.7). Figure 3 shows a plot of the ratio W_L/Γ, in the large-Γ regime, for several values of the restitution coefficient α. It is worth noticing that the lower bound $\tau_{\min}$ of the locking region increases regularly from $\tau_{\min}=0.284\,852$ for $\alpha=0$ to $\tau_{\min}=\frac{1}{2}$ as $\alpha\to 1$, in agreement with the above analytical predictions (3.13) and (3.16).

D. Towards a global description of trajectories

1. *Why typical trajectories are eventually periodic*

The essential outcomes obtained so far in this section are as follows. Consider a typical trajectory of the partially inelastic ball, with $0<\alpha<1$. First, the relative takeoff velocities W_k are bounded by $W_{\max}$. We have, in Eqs. (3.3) and (3.6), provided a rough estimate of this quantity, which describes the main features of its α and Γ dependence, and have already noted that $W_{\max}$ is a measure of the accessible volume of phase space.

On the other hand, for arbitrary values of the control parameters α and Γ, there is a region of phase space, defined as $W<W_L(\tau)$, which corresponds to complete chattering, or locking. A trajectory entering this region undergoes an infinite series of chattering bounces, in decaying geometrical progression. The ball will then wait until it is relaunched at the beginning of the next platform cycle, with the following initial conditions:

$$\tau_0=\frac{1}{2\pi}\arcsin\frac{1}{\pi\Gamma},\quad W_0=0\ . \tag{3.17}$$

The memory of the past history is thus entirely lost after a "locking encounter," *just as in the completely inelastic case* [15].

We can then argue as follows, aiming for a qualitative physical picture rather than a demonstration of mathematical rigor. A typical trajectory will explore its whole phase space and end up in the locking region after a finite number of collisions. The ball will therefore be relaunched with the initial conditions (3.17) and end up again in the locking region; this process will repeat itself periodically.

We thus arrive at the unavoidable conclusion that *a generic trajectory of the partially elastic bouncing ball is eventually periodic,* after a transient regime extending up to its first passage through locking. In other words, and from a qualitative viewpoint, the situation in the partially elastic case ($0<\alpha<1$) is not too different from that of the completely inelastic problem ($\alpha=0$). The main quantitative influence of a finite restitution coefficient is that the mean period is lengthened so as to diverge as the elastic limit is reached; this will become clear below. The above heuristic argument has been checked by means of a numerical solution of the dynamical equations (2.5)–(2.7). We will deal with quantitative aspects later in this section.

2. *Modulated structure of phase portraits*

It turns out that the reduced phase space is not filled uniformly by typical long trajectories, but rather that phase portraits show an interesting modulated structure. By solving numerically the dynamical equations (2.5)–(2.7), we have generated very long trajectories, with more than 10^4 collisions. Figure 4 shows phase por-

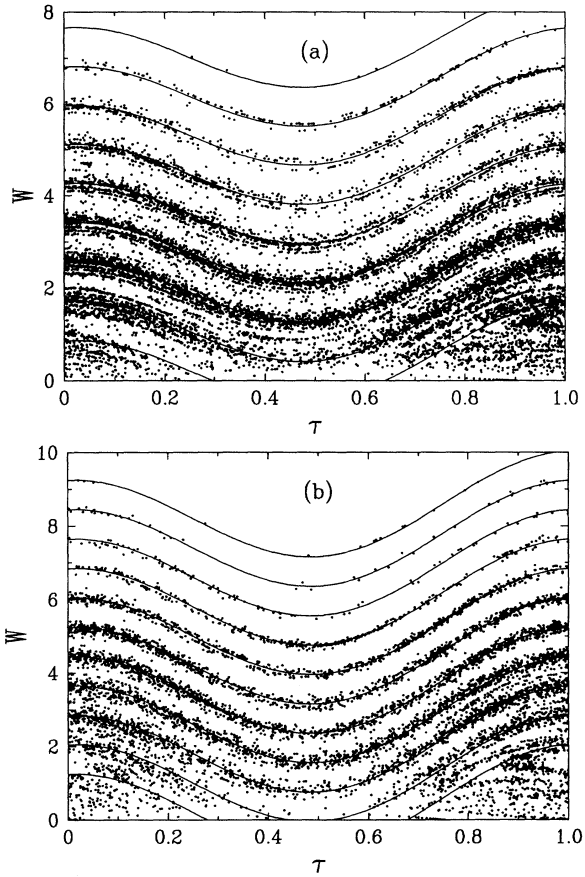

FIG. 4. Scatter plot of two typical trajectories in reduced phase space (W against τ). These "phase portraits" show the clustering of the W values around the modulated spiraling line (3.18). Parameters are as follows: (a) $\alpha=0.85$, $\Gamma=1.005$; (b) $\alpha=0.8$, $\Gamma=1.5485$.

traits, i.e., scatter plots in reduced phase space ($0 \le \tau < 1; W > 0$), of two typical examples of such long trajectories.

The points, representing the successive ball-platform collisions, are highly nonuniform in the W direction, but they cluster around the following line spiraling around the cylindrical phase space:

$$W \approx \alpha[\tau + n + \Gamma \cos(2\pi\tau)] , \tag{3.18}$$

where n is an arbitrary integer which takes account of the compactification of the τ variable. The clustering effect is more pronounced for higher values of W, whereas the lower part of phase space seems to be explored in a more uniform and "random" way.

The law (3.18) can be understood as follows. The dynamical equations (2.5)–(2.7) imply

$$W_1 = \alpha\{2(\tau_1 - \tau_0) - W_0 + \Gamma[\cos(2\pi\tau_1) - \cos(2\pi\tau_0)]\} . \tag{3.19}$$

This formula exhibits a strong τ_0 and W_0 dependence, whereas we are looking after an intrinsic description of the dynamical correlations between τ_1 and W_1, irrespective of the history of the trajectory. Most of the unwanted dependence can be eliminated by utilizing the high-bounce approximation (3.7). We are thus left with the estimate

$$W_1 \approx \alpha[\tau_1 + \Gamma \cos(2\pi\tau_1) - \tau_0] . \tag{3.20}$$

A few comments are in order. First, the high-bounce approximation can only be accurate when relative velocities are rather large. This is in agreement with the numerical observations, namely that the modulation is more prominent in the upper half of the phase portraits. Second, the estimate (3.20) still involves a weak explicit τ_0 dependence, which is also compatible with the observations. Indeed, for moderate values of W, the spiraling line (3.18) shows the trend of a periodic modulation, reflecting the τ_0 dependence. Furthermore, very large W values are most probably generated by the highest bounces, which correspond to $\tau_0 \approx 0$. This explains why the data points lie very accurately on the spiraling line near the top of the phase portraits.

From the estimate (3.6) of $W_{\max}$, the number of occupied branches of the spiral scales as

$$n_{\max} \sim \frac{4\Gamma}{1-\alpha} \quad (\alpha \to 1) . \tag{3.21}$$

This law is confirmed by numerical data, even for values of Γ of order unity, such as those presented in Fig. 4. The prefactor of the estimate in the right-hand side of Eq. (3.21) lies between 1 and 2, i.e., it is less than half the number (4) predicted by Eq. (3.6).

3. *Quantitative statistical aspects*

We end this section devoted to global aspects of the dynamics by presenting some quantitative statistical predictions concerning the typical period of a trajectory and comparing them with the outcome of extensive numerical work.

Consider a trajectory defined by the initial conditions (3.17), with "generic" values of the control parameters α and Γ. We know that the trajectory will enter the locking region after some number N of ball-platform collisions, i.e., $W_{N-1} > W_L(\tau_{N-1})$ but $W_N \le W_L(\tau_N)$. It will then undergo locking, which involves an infinite series of collisions in a finite time interval.

This effect makes it difficult to attach simple quantitative estimates to trajectories in an unambiguous way, such as the winding number used extensively in Ref. [15].

The period $\mathcal{T}$ of a trajectory is a more meaningful concept, as is the number N of its collisions outside the locking region. More precisely, the period is defined as $\mathcal{T} = 1 + \mathrm{int}(\tau_N)$, where τ_N is the first time for which the ball, launched initially according to Eq. (3.17), enters the locking region.

We will argue in a while that the distribution of the random observables N and $\mathcal{T}$ is Poissonnian, at least near the elastic limit ($\alpha \to 1$). The physical meaning of such statistical statements in the present context is the following. Consider an ensemble of trajectories defined by the initial conditions (3.17), for many different values of the parameter Γ, chosen, e.g., to be equally spaced over a narrow interval of the form $[\Gamma_0 - \Delta\Gamma, \Gamma_0 + \Delta\Gamma]$. The statistical predictions to be described below are meant to apply to averages over such ensembles of trajectories. The numerical data discussed hereafter have to be interpreted within this framework.

Let us hypothesize that there is a small probability p that the trajectory enters the locking region of phase space at any ball-platform collision. We will refer to p as the locking probability, which depends a *priori* on α and Γ.

A first very rough estimate for the locking probability p can be derived by assuming that the invariant measure is approximately uniform over the accessible volume of phase space: p can then be estimated as the following ratio of phase-space volumes

$$p_{\text{uniform}} = \frac{\overline{W}_L}{W_{\max}} , \tag{3.22}$$

with

$$\overline{W}_L = \int_0^1 W_L(\tau_0) d\tau_0 . \tag{3.23}$$

The above estimates yield the following predictions for the α and Γ dependence of the locking probability.

In the strongly inelastic regime ($\alpha \to 0$), Eq. (3.13) leads to $\overline{W}_L \approx q\Gamma$, where $q \equiv 0.418\,847$ is evaluated by numerical integration. A comparison with Eq. (3.6) shows that $p_{\text{uniform}} \approx 1$ for $\alpha \approx q/4 \approx 0.10$. This means that for such values of α, the effects of the locking region become quite similar to those of the absorbing region for $\alpha = 0$.

In the opposite regime where the elastic limit is approached ($\alpha \to 1$), the estimate (3.16) implies that p_{uniform} vanishes according to

$$p_{\text{uniform}} \approx \frac{(1-\alpha)^2}{16} , \tag{3.24}$$

independently of Γ.

In the following, we consider mostly large values of the

restitution coefficient ($\alpha \to 1$). We assume that there is a small stationary locking probability p, which is independent of Γ at least in the large-Γ regime, in qualitative accord with the estimate (3.24).

This hypothesis implies Poisson statistics for the finite number N of "strong" ball-platform collisions per period, i.e., the collisions which take place before the ball enters the locking region. Indeed, neglecting any dynamical correlations between different collisions, we can estimate as follows the probability π_N that a trajectory enters the locking region exactly at the Nth ball-platform collision:

$$\pi_N = p(1-p)^{N-1} \approx p \exp(-Np) \ . \tag{3.25}$$

As a consequence, the average and the root-mean-square value of the number of collisions per period outside the locking region read

$$N_{\rm av} = \sum_{N=1}^{\infty} N \pi_N \approx \frac{1}{p} \ ,$$
$$N_{\rm rms} = \left[\sum_{N=1}^{\infty} N^2 \pi_N - N_{\rm av}^2 \right]^{1/2} \approx \frac{1}{p} \ . \tag{3.26}$$

Moreover, since a finite proportion of the flights can be described, at least in a qualitative way, by the high-bounce approximation (3.7), we can infer that the period $\mathcal{T}$ of the ball's history possesses the same kind of distribution as $N\Gamma$ in the large-Γ regime, namely

$$\mathcal{T}_{\rm av} \approx \mathcal{T}_{\rm rms} \approx \frac{c\Gamma}{p} \ , \tag{3.27}$$

where c is a constant.

We have performed extensive numerical checks of the above heuristic ideas; we have measured the mean and the rms value of the period $\mathcal{T}$ of trajectories started with the initial conditions (3.17), with equally spaced values of Γ in the interval $[\Gamma_0 - \Delta\Gamma, \Gamma_0 + \Delta\Gamma]$, for $\Delta\Gamma = 0.5$ and $\Gamma_0 = 7.5, 15$. Our results are illustrated in Fig. 5, which is a log-log plot of the ratios $\mathcal{T}_{\rm av}/\Gamma$ and $\mathcal{T}_{\rm rms}/\Gamma$ against $(1-\alpha)$. Each data point corresponds to 10^3 trajectories. The following aspects of the above discussion are corroborated convincingly: (1) The data points for the mean and rms values of the period almost coincide, thus confirming Poissonian behavior (3.25) and (3.26); (2) both series of data fall onto one single curve once the parameter Γ_0 has been divided out; and (3) the scaling curve is very close to being straight. The full line shown on the plot has a slope 5, evaluated by means of a least-square fit to the data with $\alpha \geq 0.60$. We have thus confirmed the main predictions of the above discussion and obtained the following *critical behavior:*

$$\mathcal{T}_{\rm av} \approx \mathcal{T}_{\rm rms} \approx C\Gamma(1-\alpha)^{-\nu}, \quad \nu \approx 5, \ C \approx 1.9 \tag{3.28}$$

for the mean period as the elastic regime is approached.

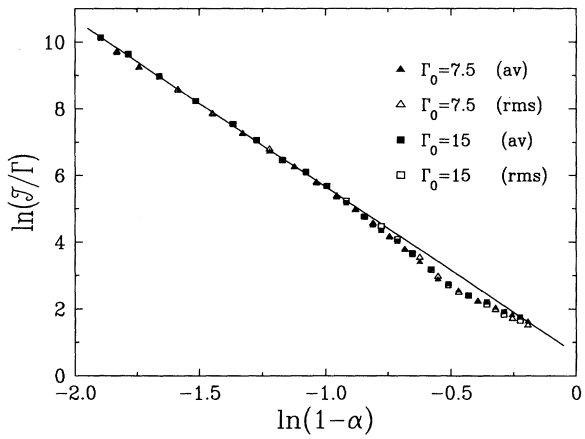

FIG. 5. Log-log plot of the mean and rms values of the period $\mathcal{T}$ against $(1-\alpha)$. Two ensembles of 10^3 trajectories each, such that $\Gamma_0 - \Delta\Gamma < \Gamma < \Gamma_0 + \Delta\Gamma$, with $\Delta\Gamma = 0.5$, and $\Gamma_0 = 7.5$ and $\Gamma_0 = 15$, have been used for every value of α. The straight line shows the fit of Eq. (3.28), implying that the typical period scales as the power law $\mathcal{T} \sim \Gamma(1-\alpha)^{-\nu}$, with $\nu \approx 5$.

Both the power-law form of Eq. (3.28) and its Γ dependence are in qualitative accord with the above heuristic estimates. Our fitted numerical value of the *critical exponent* ν is more than twice as large as the naive estimate $\nu = 2$ of Eq. (3.24), corresponding to a uniform invariant measure; this confirms the heuristic statistical description proposed above, which, rather than an accurate determination of exponents, was the object of our exercise.

We are thus left with the following physical picture of a typical history of the ball in the nearly elastic situation ($\alpha \to 1$) and in the large-Γ regime. A generic trajectory will consist of a large number [of order $N \sim (1-\alpha)^{-\nu}$] of ball-platform collisions, with $\nu \approx 5$, before it enters the locking region; it will then become periodic in time. The associated temporal period is typically of order $\mathcal{T} \sim \Gamma(1-\alpha)^{-\nu}$.

IV. DISCUSSION AND CONCLUSIONS

We have presented a detailed study of the bouncing ball with finite restitution. One of the most surprising aspects of our work has been to show that the dynamics of the completely inelastic ball ($\alpha = 0$), investigated in earlier work [15], remains a good qualitative indicator for the dynamics of the ball with finite restitution up to values of α close to 1, whereas a naive application of intuition might suggest that the crossover to fully chaotic behavior should occur for much smaller values of α.

More precisely, because of the existence of a complete chattering, or locking, region in phase space, a generic trajectory starting under experimental conditions, namely at rest, will repeat itself in a periodic way. The mean period and the mean number of rebounds have been shown to exhibit critical behavior as the elastic limit is approached, namely to diverge as the power law $(1-\alpha)^{-\nu}$. An extensive numerical study has led us to the estimate $\nu \approx 5$.

As a consequence, we believe that the experimental observation of chaos [7,11], especially for α close to unity, is due to experimental limitations to date which have made for an insufficiently sharp distinction between long trajectories which are ultimately periodic and those which would exhibit a true chaotic evolution. Of course, the experimental distinction between periodic and chaotic evolution rapidly becomes academic as $\alpha \to 1$, since the pre-

dicted mean period grows beyond experimental reach. A good experimental check of the present theory would be an experiment performed on a "pointlike" bouncing ball (so that one could neglect tensorial aspects in its elasticity), for long enough observation times that the distinction between truly chaotic and ultimately periodic trajectories could be made precise.

There are, however, still many unanswered interesting questions. Chief among those is the detailed investigation of the region of partial transmission, i.e., the region where the ball manages to escape into the next transmitting region via the process of incomplete chattering: $W_L(\tau) < W < W_A(\tau)$. This region of phase space, represented by the area between the graphs of W_L/Γ and W_A/Γ in Fig. 2, is rather small near $\alpha=0$. This justifies the approach of our earlier work on the $\alpha=0$ case, where we have divided phase space into a completely transmitting and a completely absorbing region.

For larger values of the restitution coefficient, between $\alpha \approx 0.1$ and $\alpha \to 1$, incomplete chattering becomes progressively more frequent for typical trajectories, as shown in Fig. 3. It would be interesting to see the full quantitative effect of this admittedly small region of phase space. While we do not expect a more detailed study to alter drastically the conclusions presented in this paper, it could shed some light on questions such as the invariant measure in phase space and the value of the exponent ν. Also, such an investigation could help resolve the issue of the extension of the definition of the winding number presented in Ref. [15] and analyze in particular the discontinuities of that quantity as a function of α and Γ.

Another open question is that of the period-doubling sequence. We have shown why this route to chaos is not observable for "physical" trajectories. A better understanding of the size of its basin of attraction in phase space, at least for the rescaled form of the dynamical equations, i.e., the Hénon map with negative b, would be a worthwhile goal.

In conclusion, we have shown that the nature of the dynamics of the bouncing ball with finite restitution is far from simple, contrary to earlier assumptions. It is our hope that some of the questions we have raised, especially those relating to chattering and locking, and their nontrivial implications for the evolution to chaos in this deceptively simple system, will form the basis of detailed theoretical and experimental work in the future.

ACKNOWLEDGMENT

A.M. acknowledges the hospitality of the Service de Physique Théorique, where most of this work was carried out.

*Electronic address: luck@amoco.saclay.cea.fr
†Electronic address: a.mehta@birmingham.ac.uk

[1] E. Fermi, Phys. Rev. **75**, 1169 (1949).
[2] L. D. Pustylnikov, Trans. Moscow Math. Soc. **2**, 1 (1978).
[3] G. M. Zaslavskii, Phys. Lett. **69A**, 145 (1978).
[4] B. V. Chirikov, Phys. Rep. **52**, 263 (1979).
[5] A. J. Lichtenberg, M. A. Lieberman, and R. H. Cohen, Physica D **1**, 291 (1980).
[6] J. Guckenheimer and P. J. Holmes, J. Sound Vib. **84**, 173 (1982).
[7] P. Pieranski, J. Phys. (Paris) **44**, 573 (1983); P. Pieranski, Z. J. Kowalik, and M. Franaszek, *ibid.* **46**, 681 (1985); P. Pieranski and R. Bartolino, *ibid.* **46**, 687 (1985); P. Pieranski, Phys. Rev. A **37**, 1782 (1988); Z. J. Kowalik, M. Franaszek, and P. Pieranski, *ibid.* **37**, 4016 (1988).
[8] N. B. Tufillaro and A. M. Albano, Am. J. Phys. **54**, 939 (1986).
[9] R. M. Everson, Physica D **19**, 355 (1986).
[10] S. Celaschi and R. L. Zimmerman, Phys. Lett. A **120**, 447 (1987).
[11] T. M. Mello and N. B. Tufillaro, Am. J. Phys. **55**, 316 (1987).
[12] A. B. Pippard, Eur. J. Phys. **8**, 203 (1987).
[13] K. Wiesenfeld and N. B. Tufillaro, Physica D **26**, 321 (1987).
[14] G. A. Luna-Acosta, Phys. Rev. A **42**, 7155 (1990).
[15] A. Mehta and J. M. Luck, Phys. Rev. Lett. **65**, 393 (1990); Mod. Phys. Lett. B **4**, 1245 (1990).
[16] M. Hénon, Commun. Math. Phys. **50**, 69 (1976).
[17] J. P. Eckmann and D. Ruelle, Rev. Mod. Phys. **57**, 617 (1985).
[18] P. Collet and J. P. Eckmann, *Iterated Maps on the Interval as Dynamical Systems* (Birkhäuser, Boston, 1980).
[19] M. J. Feigenbaum, J. Stat. Phys. **19**, 25 (1978); **21**, 669 (1979); Phys. Lett. **74A**, 375 (1979).